Traveling-cluster approximation for uncorrelated amorphous systems

Asok K. Sen and Robert Mills
Department of Physics, The Ohio State University, Columbus, Ohio 43210

Theodore Kaplan
Solid State Division, Oak Ridge National Laboratory, Oak Ridge, Tennessee 37830

L. J. Gray
Engineering Physics and Mathematics Division, Oak Ridge National Laboratory, Oak Ridge, Tennessee 37830
(Received 29 February 1984)

We have developed a formalism for including cluster effects in the one-electron Green's function for a positionally disordered (liquid or amorphous) system without any correlation among the scattering sites. This method is an extension of the technique known as the traveling-cluster approximation (TCA) originally obtained and applied to a substitutional alloy by Mills and Ratanavararaksa. We have also proved the appropriate fixed-point theorem, which guarantees, for a bounded local potential, that the self-consistent equations always converge upon iteration to a unique, Herglotz solution. To our knowledge, this is the only analytic theory for considering cluster effects. Furthermore, we have performed some computer calculations in the pair TCA, for the model case of δ-function potentials on a one-dimensional random chain. These results have been compared with "exact calculations" (which, in principle, take into account all cluster effects) and with the coherent-potential approximation (CPA), which is the single-site TCA. The density of states for the pair TCA clearly shows some improvement over the CPA and yet, apparently, the pair approximation distorts some of the features of the exact results.

I. INTRODUCTION

The properties of electronic states for a spatially disordered system, after many years of study, are still not well understood. On one hand, there have been exact, or nearly exact, numerical studies, in which the actual states are counted for finite, randomly chosen, one-dimensional samples[1–4] to obtain the integrated density of states. These results, which can be described as "computer experiments," can be used to demonstrate the success or failure of theories developed to understand the physics of such systems. [It may be mentioned here that there is very little experimental data with which to compare theoretical predictions about densities of states (DOS).] On the other hand, there are analytical methods[5–9] which start from the one-electron Hamiltonian and make some approximations to obtain the configuration-averaged Green's function. Usually, these theories do not try to look at the effects of vibrations of the scatterers on the electronic density of states (electron-phonon interactions). Also, in most of them the electron-electron interaction and the consequent screening effects are neglected. Our presentation falls in the category of analytical approximation methods. There are two important aspects of the problem to be considered. The first is the effect of local clusters of scatterers (regardless of correlations), and the second is the effect of correlations (or short-range order). In each case, it is particularly important to preserve the Herglotz property of the averaged Green's function, which is the set of analyticity properties (see Ref. 10) that are necessary to ensure causality and a non-negative, single-valued density of states.

The time-honored "coherent-potential approximation"[11] (CPA) is a single-site approximation (that is, it does not include scattering from clusters in the perturbative expansion of the full Green's function) developed for substitutional alloys, that preserves the Herglotz property. The application of the CPA logic to liquids due to Klauder[7] and Faulkner,[5] also has the Herglotz property, as demonstrated in this paper, but like the substitutional CPA does not take into account short-range order. The effective medium approximation (EMA) of Roth and others[6,8,9] is also a single-site approximation, which deals with short-range order by means of an approximate expression for the n-scatterer correlation function in terms of the pair correlation function. Like almost all other ways of including short-range order, the EMA fails to preserve the Herglotz property, but nevertheless gives quite reasonable results in many instances. Progress made in this direction may be found in some recent works of Nicholson and others.[12–14] Singh[9] has devised an ingenious modification of the EMA which seems somewhat contrived but which preserves the Herglotz property and gives quite nice numerical results.

Of the efforts to include cluster scattering in random substitutional alloys, there are two extensions of the CPA that preserve the Herglotz property and translational symmetry, the traveling-cluster approximation (TCA) of Mills and Ratanavararaksa[10] (which we will refer to as MR) and the generalization of the TCA to off-diagonal and environmental disorder by Kaplan, Leath, Gray, and Diehl[15] (KLGD). The TCA retains translational symmetry and

achieves the Herglotz property by the inclusion of large classes of cumulant average graphs. It can be described as the analytic completion of the m-site CPA.[16,17] KLGD similarly achieves proper translational symmetry and the Herglotz property while extending the cluster approximation to general Hamiltonians by paralleling the TCA development in the augmented space formalism.[15,18,19] The major shortcoming of these approximations is that short-range order cannot be treated fully self-consistently but rather only in a perturbation expansion of the uncorrelated solution.[20]

In this paper, we apply the TCA concepts to spatially disordered, uncorrelated systems, e.g., fluids or amorphous metals without short-range order. We believe that this is the first approximation scheme for amorphous systems that takes cluster effects into account while preserving the Herglotz property for any amount of disorder. It is the natural extension, with inclusion of cluster effects, of the Klauder-Faulkner CPA. It is our hope that this is a step toward the goal of a systematic cluster approximation for amorphous systems that includes short-range order and also preserves the Herglotz property.

The presentation of the paper is as follows. In Sec. II, we develop the set of self-consistent equations that need to be solved for a pair theory. This we do without trying to be general and without introducing the more abstract formalism. In Sec. III, we solve these equations for the model case of a one-dimensional liquid with δ-function potentials at the scattering centers, so that we can compare our approximation with the exact results that are available only for this case, and with the CPA.

To be able to study the nature of the TCA at the formal level, it is convenient to express the configuration average as the "ground-state" expectation value of suitable resolvent operator in a much larger vector space called the augmented space.[10,15,18,19] In Appendix A, we construct the augmented space for a liquid and show how to develop the fluid TCA in this framework. This gives a formal expression for the coherent potential for any finite-order TCA which is then used in Appendix B to prove the relevant fixed-point theorem. Assuming that the initial approximation for the coherent potential has the Herglotz property, the coherent potential obtained at any stage of iteration of the self-consistent equations also has the Herglotz property, while the iterative process itself necessarily converges to a unique, self-consistent, Herglotz solution as the number of iterations goes to infinity.

II. TCA FOR UNCORRELATED FLUIDS: PAIR APPROXIMATION

In a fluid or, in general, in a positionally disordered (amorphous) system, the Hamiltonian for an electron has the form

$$H=H_0+V\ , \tag{2.1}$$

$$V=\sum_{i=1}^{N} V_i\ , \tag{2.2}$$

where H_0 is the nonrandom part of the Hamiltonian and V_i is the potential due to a scatterer at the random position x_i. V_i is taken to be localized, centered at x_i:

$$\langle r \mid V_i \mid r' \rangle = \delta(r-r')v(r-x_i)\ , \tag{2.3}$$

where v is the same for all the scatterers. The scattering sites x_i are taken to be uncorrelated with density n. We seek an approximation to the mean resolvent, or average Green's function G^c, defined as

$$G^c=\langle (E-H)^{-1}\rangle \tag{2.4}$$

$$=(L_0-V^c)^{-1}\ , \tag{2.5}$$

where E is the complex energy variable,

$$L_0=E-H_0=(G^0)^{-1}\ , \tag{2.6}$$

and V^c, defined by Eq. (2.5), is called the "coherent potential."

Now, in a fluid, as opposed to a substitutional alloy, each site may be anywhere in the whole volume, with the consequence that the modified cumulant average (MCA) is identical to the cumulant average (CA). [Mills and Ratanavararaksa (Ref. 10); Mills (Ref. 17).] To see this, recall first that the MCA (see MR) of a given order m, associated with a site i, is the sum of all the mth-order CA graphs involving overlapping CA's associated with the site i. The presence of interactions at other sites interspersed among the m interactions at site i does not affect this definition. This is illustrated in the fourth order in Fig. 1(a). However, the volume dependence of the different terms depends on the number of distinct CA's, with the result that in the infinite-volume limit only the leading term, consisting of a single mth-order CA, survives [Fig. 1(b)], as explained in detail but in different language, in Ref. 17. Thus, the expansion for a fluid or amorphous material can be seen as a CA expansion in which no CA's associated with a single site i are allowed to overlap.

The contribution $(V^c)^{(1)}$ to V^c corresponding to Fig. 1 is given by

$$(V^c)^{(1)}=n\int dx\, V_x G^0 V_x G^0 V_x G^0 V_x\ , \tag{2.7}$$

where n is the density of scatterers and each single MCA line is associated with a factor n. In keeping with the notation introduced in MR, in the MCA graphs the electron line is not shown [as on the left-hand side of Fig. 1(a)] since it carries no useful information.

The terms in the MCA expansion can be characterized by the different sets of sites referred to as "overlap sets," involved in each place where MCA lines overlap. A given approximation in the TCA consists of the sum of all terms in which the overlap sets are restricted to some family T of sets that characterizes the approximation. For the substitutional alloy, the simplest approximation beyond the CPA is that for which T consists of all single-site sets and all nearest-neighbor pairs. In the fluid

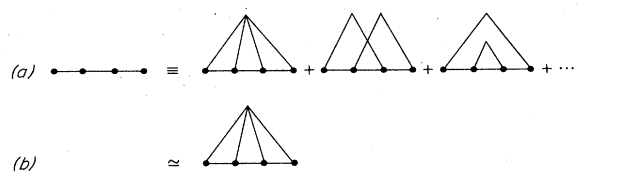

FIG. 1. MCA graphs reduce to CA graphs in the infinite volume limit.

TCA, degree of "neighborliness" is not so conveniently defined, and the simplest approximation beyond the CPA is that for which T includes, in addition to the single-site sets, all pairs regardless of separation. Some typical terms are shown in Fig. 2.

Now, this way of truncating the expansion, corresponding to the diagrams indicated in Fig. 2, yields a non-self-consistent approximation if between any two successive scatterings the propagator G^0 is used. To achieve self-consistency in the (non-Herglotz[21]) m-site CPA (see Ref. 17), one simply sums over irreducible graphs while replacing G^0 by G^c. In the general m-site TCA, on the other hand, the MCA expansion explicitly includes reducible terms, and thus replacing G^0 by G^c would lead to overcounting of graphs. The prescription obtained by MR for alloys requires inserting a different self-consistent propagator $G^{(S)}$ for each different overlap set S. To avoid overcounting, it is necessary that each self-energy graph included in $V^{(S)}$ (the self-energy corresponding to $G^{(S)}$) begin and end on sites i and j such that the sets $S \cup \{i\}$ and $S \cup \{j\}$ do not belong to the family T of allowed overlap sets defining the approximation. The fluid TCA, however, includes in T *all* sets of sites up to a specified order m, with the result that $G^{(S)}$ reduces to G^0, if S is of order less than m, while $G^{(S)}$ becomes the full mean resolvent G^c if S is of order m.

A formal expression for G^c in a given approximation TCA(m) in the augmented space formalism is obtained in Appendix A. This form is particularly useful in proving the related fixed-point theorem, which says (1) that at any stage of iteration of the self-consistent set of equations, G^c will be Herglotz (see MR), provided only that it is initially chosen to be so, and (2) that for any complex E, the process of iteration converges to a unique physical solution. It may be reiterated here that if the solution for $G^c(E)$ is not Herglotz, then its time Fourier transform $G^c(t)$ is not causal, and the density of states may become negative and/or nonunique.[21] The fixed-point theorm for the fluid TCA is proved in Appendix B.

For the purpose of demonstrating the nature of the fluid TCA, we now have to formulate the problem at a calculational level. For computational feasibility and to permit comparison with "exact" results, we have carried out the two-site TCA for a 1D liquid with δ-function potentials of strength v. The structure of the calculation is suggested by Fig. 3, in which a typical graph is broken down into different types of overlap regions. Thus, e and f represent two different types of overlap regions, that is, e is the sum of all two-site overlap contributions that begin and end at the same site, while f is the sum of terms that begin and end on different sites as explained in Fig. 3. The self-consistent propagator in the overlap regions is the full average Green's function G^c, while in single-site regions it must be G^0, the free electron Green's function, to avoid overcounting. The functions e and f satisfy simultaneous algebraic equations displayed pictorially in Figs. 4(a) and 4(b). Thus,

$$e(\xi)=nv+vG^c(0)e(\xi)+vG^c(\xi)f(\xi)\ , \tag{2.8}$$

$$f(\xi)=vG^c(-\xi)e(\xi)+vG^c(0)f(\xi)\ . \tag{2.9}$$

Of course,

$$G^c(\xi)=G^c(-\xi)\ . \tag{2.10}$$

We solve and get

$$e(\xi)=nv[1-vG^c(0)]/\Delta(\xi)\ , \tag{2.11}$$

$$f(\xi)=nv^2G^c(-\xi)/\Delta(\xi)\ , \tag{2.12}$$

$$\Delta(\xi)=[1-vG^c(0)]^2-v^2G^c(\xi)G^c(-\xi)\ . \tag{2.13}$$

Next, V^c is expressed in terms of its initial and final scatterings as represented in Fig. 5(a):

$$V^c(x-y)=nv\delta(x-y)+nv^2\mathscr{g}(0,0;x-y)\ , \tag{2.14}$$

where $\mathscr{g}(\xi,\eta;x-y)$ represents graphs where y and x are the initial and final scatterer locations, and $y+\eta$ and $x+\xi$ are the initial and final electron locations. As shown in Fig. 5(b), $\mathscr{g}$ satisfies

$$\mathscr{g}(\xi,\eta;x-y)=G^0(\xi-\eta)\delta(x-y)+vG^0(\xi)\mathscr{g}(0,\eta;x-y)+\int G^0(\xi-\xi')e(\xi')\mathscr{g}(\xi',\eta;x-y)d\xi' + \int G^0(\xi+\xi')f(\xi')\mathscr{g}(\xi',\eta;x-\xi'-y)d\xi'\ . \tag{2.15}$$

In fact, we need $\mathscr{g}$ only for $\eta=0$. We now Fourier transform in $x-y$, to obtain

$$\mathscr{g}(\xi,0;k)=\int e^{-ikx}\mathscr{g}(\xi,0;x)dx =G^0(\xi)[1+v\mathscr{g}(0,0;k)]+\int d\xi' G^0(\xi-\xi')e(\xi')\mathscr{g}(\xi',0;k)+\int d\xi' G^0(\xi+\xi')f(\xi')e^{-ik\xi'}\mathscr{g}(\xi',0;k)\ , \tag{2.16}$$

$$V^c(k)=\int e^{-ikx}V^c(x)dx=nv+nv^2\mathscr{g}(0,0;k)\ , \tag{2.17}$$

and

$$G^c(k)=\frac{1}{E-k^2-V^c(k)}\ , \tag{2.18}$$

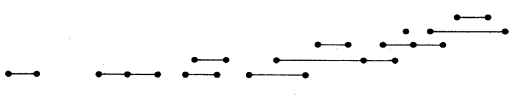

FIG. 2. Typical contributions to V^c in the two-site TCA. Only one- and two-site overlap sets are allowed.

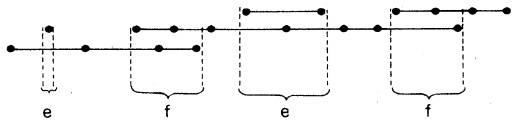

FIG. 3. A typical V^c graph broken up into distinct overlap regions e and f.

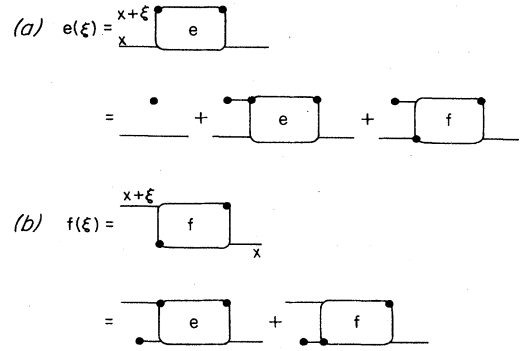

FIG. 4. Diagrammatic representation of overlap regions (a) $e(\xi)$, and (b) $f(\xi)$.

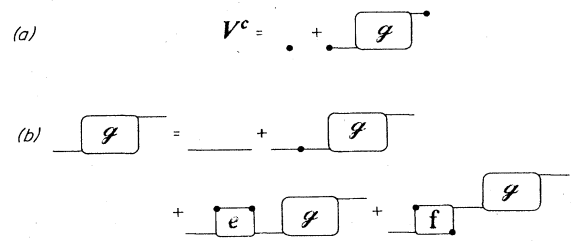

FIG. 5. Diagrammatic representation of the coherent potential V^c in TCA(2).

where our units are such that $\hbar^2/2m=1$. It may be mentioned here that two of us (T.K. and L.J.G.) obtained the same set of equations as above by starting from the augmented space formulation (as given in Appendix A) for a family of up to pair clusters and using a (nondiagrammatic expansion) method analogous to that presented in KLGD.[15]

III. MODEL CALCULATIONS AND DISCUSSIONS OF RESULTS

For machine calculations of the electronic density of states of one-dimensional amorphous or liquid metals with δ-function potentials, we start from Eq. (2.16), and cut off the integrals on the right-hand site at $\xi=x_0$. This would be strictly valid if $e(\xi)$ and $f(\xi)$ vanished identically beyond $\xi=x_0$, and should be reasonable if they become small beyond x_0. On the assumption that $G^c(\xi)\to 0$ for large ξ, we see from Eq. (2.11) that, while $f(\xi)\to 0$, $e(\xi)$ approaches a constant value,

$$e(\xi)\to e(\infty)=\frac{nv}{1-vG^c(0)} . \tag{3.1}$$

Defining a renormalized $e^R(\xi)$, which does vanish at $\xi=\infty$, by

$$e^R(\xi)=e(\xi)-e(\infty) \tag{3.2}$$

and a renormalized Green's function,

$$(G^0)^R=[(G^0)^{-1}-e(\infty)]^{-1}=(E^R-H_0)^{-1} , \tag{3.3}$$

where

$$E^R=E-e(\infty) , \tag{3.4}$$

we can rewrite the integral equation in a form which is valid if e^R and f are sufficiently small for $\xi>x_0$:

$$\mathcal{G}(\xi,0;k)=[G^0(\xi)]^R[1+v\mathcal{G}(0,0;k)]+\int_{-x_0}^{x_0} d\xi'\{[G^0(\xi-\xi')]^R e^R(\xi')+[G^0(\xi+\xi')]^R f(\xi')e^{-ik\xi'}\}\mathcal{G}(\xi',0;k) . \tag{3.5}$$

The density of states, $\rho(E)$, per unit length is then calculated using the formula

$$\begin{aligned}\rho(E)&=-\frac{1}{\pi L}\mathrm{Im\,Tr}G^c\\&=-\frac{1}{\pi}\mathrm{Im}\frac{1}{2\pi}\int dk\, G^c(k,E)\\&=-\frac{1}{\pi}\mathrm{Im}[G^c(x,E)]_{x=0} .\end{aligned} \tag{3.6}$$

Computations were done, with $v=-2$, at three particle densities, $n=0.1$, 1.0, and 10.0, and compared with exact results, which were obtained using the program of Peterson, Schwartz, and Butler (Ref. 4), for the case of extremely small short-range order. The results are shown in Figs. 6–8. Comparison with single-site TCA, which is identical to the Klauder-Faulkner CPA (Refs. 5 and 7), were also done to show the importance of cluster effects.

The first thing to note is that at all the scatterer densities, the DOS extends much further in the negative energy region in the TCA(2) than in the CPA. This is somewhat to be expected from a non-self-consistent view, since an isolated dense cluster of δ functions can give a bound state of arbitrarily large negative energy. For an isolated pair of δ-function potentials of strength $v=-2$, separated by a distance x, the ground-state energy is given by $E_b=-\kappa^2$, where κ satisfies

$$1+e^{-\kappa x}=\kappa . \tag{3.7}$$

In the low-density limit, $x\gg 1$ and $E_b\simeq 1$, corresponding to the single-scatterer bound state at $E_b=-v^2/4$. In the high-density limit, $x\ll 1$ and $E_b\simeq -4$, corresponding to two δ-function potentials falling on top of each other (since there is no short-range repulsion between scatterers), which is equivalent to a single δ-function potential of strength $v'=2v=-4$. Similarly, if we take an isolated m cluster in the high-density limit, the non-self-consistent bound state is at $E_b=-(mv)^2/4$. For a cluster of three this is $E_b=-9$. In the pair TCA, then, one might expect finite densities of states for $-4\le E\le -1$, with something like a band edge at $E=-4$. It is not clear mathematically how self-consistency affects the results within or outside this energy range but one can anticipate how the exponential distribution of pair-separation length x should affect the results within the energy range. For $n=1.0$, one expects that the exponential distribution of x makes the DOS between $E=-1$ and -4 rather flat with a positive slope to close to $E=-4$. The exact results support this idea [Fig. 7(a), $n=1.0$] in contrast to the TCA(2), which shows a sharp peak at -4. When we made a non-

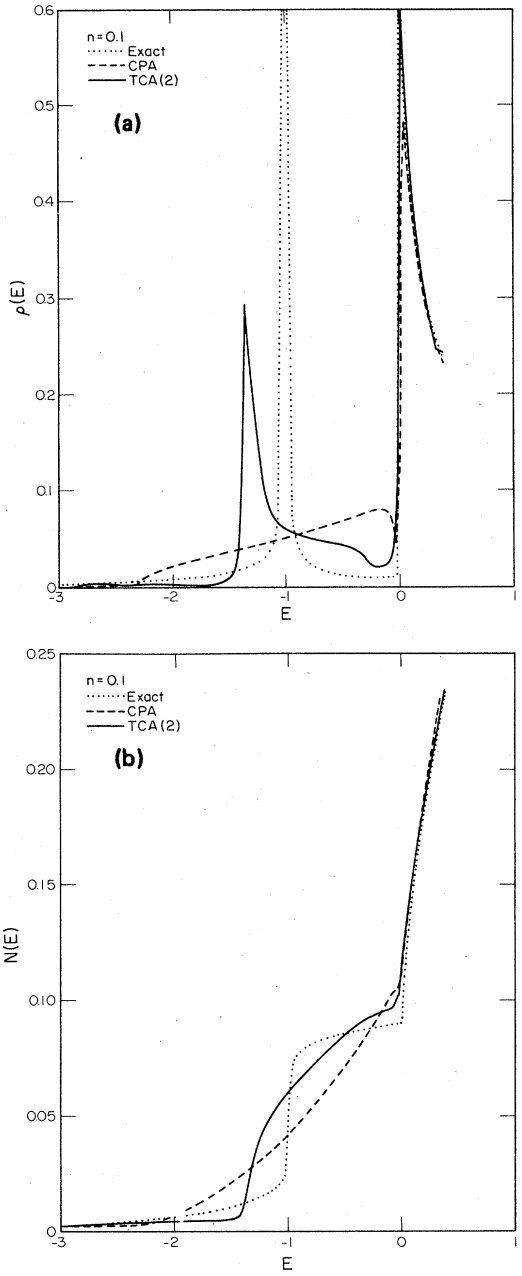

FIG. 6. (a) Differential, and (b) integrated density of states for $n=0.1$. The integrated densities are matched at $E=-2.98$.

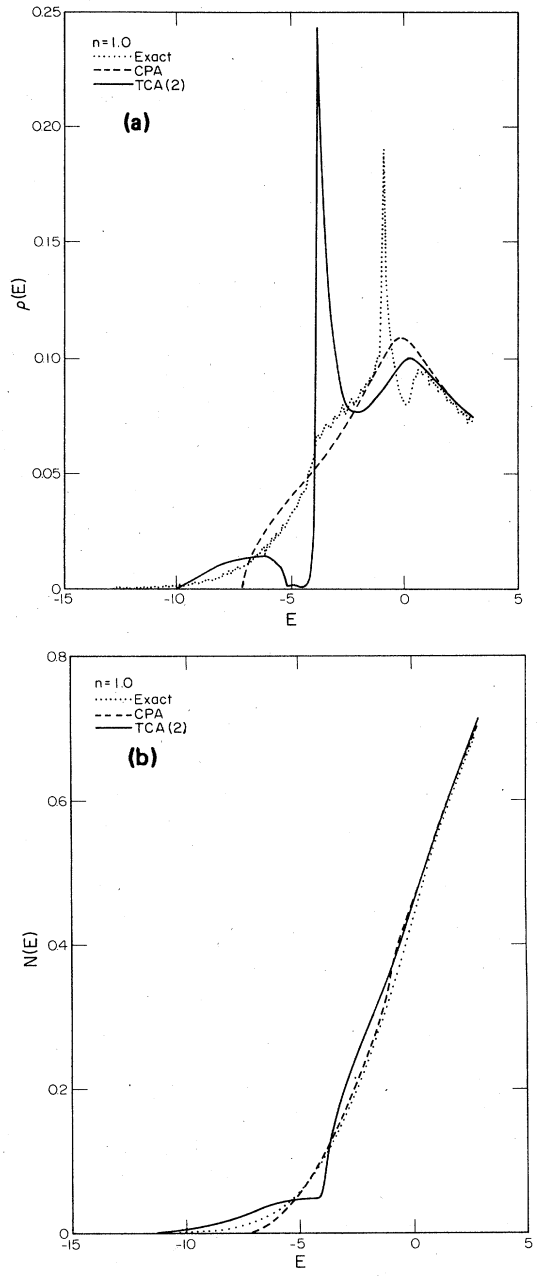

FIG. 7. (a) Differential, and (b) integrated density of states for $n=1.0$. The integrated densities are matched at $E=-11.0$.

self-consistent run of the TCA(2) program (i.e., only one interaction per energy with $G^c \rightarrow G^0$ everywhere in the program), the shape of the DOS for $n=1.0$ was very similar to the self-consistent calculation, and even quantitatively they were of the same order of magnitude. So, apparently, self-consistency is not changing anything drastically for the TCA(2). It may be mentioned in this connection that we made two tests on the program: (i) We made a non-self-consistent calculation with $e(x)=f(x)=0$ for all x at some positive energies with large imaginary parts (so that there is not much problem in Fourier transforming). This corresponds to the non-self-consistent CPA. The densities of states compared very well with results computed by hand (since the problem then is exactly solvable). (ii). We used repulsive δ-function potentials of strength $v=+2$. As expected, we found a band edge at $=0$.

Apart from removing the band edge further down in energy (for attractive potentials), the TCA(2) does some other peculiar things to the DOS. As we have seen, it tends to overemphasize the peak roughly corresponding to the bound-state energy for a pair cluster and fails to show the peak due to the single-site effect (at low densities). For example, in Fig. 7(a), for the density $n=1.0$, the exact

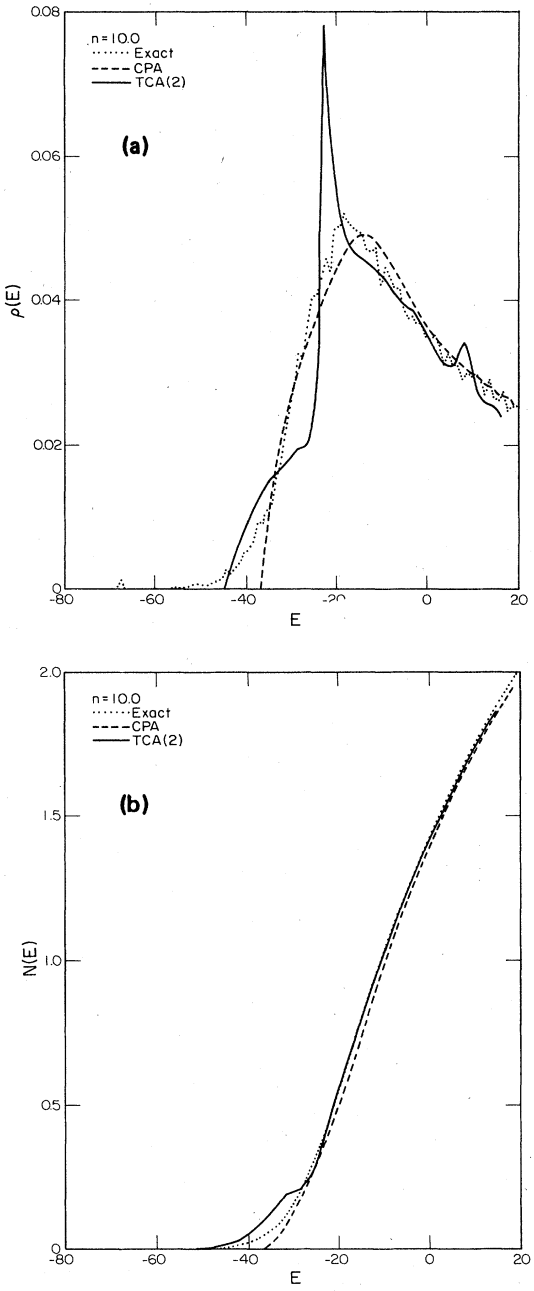

FIG. 8. (a) Differential, and (b) integrated density of states for $n=10.0$. The integrated densities are matched at $E=-67.5$.

results clearly show a peak in the DOS near $E=-4$; but it is much weaker than the single-site bound state near $E=-1$. But in the TCA(2), the peak at $E\simeq-4$ is greatly emphasized to the extent that there almost seems to be a band edge below $E=-4$, while the peak at $E=-1$ does not appear at all. In contrast to this, we may say that the CPA shows none of these peaks, at all, even though in other ways it seems to match better with the exact results. The failure of the CPA becomes more evident at lower densities, say at $n=0.1$, Figs. 6(a) and 6(b). Incidentally, we may remark that in much of the literature, the integrated DOS has been used for comparing different theories, obscuring many features that are very clear in the differential DOS, which thus gives much better insight into the success or failure of a particular theory. In any case, we have included graphs for integrated DOS, too, at all the densities. At higher densities, the difference between the exact calculation and the two approximations is much reduced, as seen in the case $n=10.0$ [Fig. 8(a)]. Again there is a sharp peak at $E\simeq-22$, but it has reduced in intensity and has moved much closer to the peak in the exact results. In short, then, we conclude that the effects of large clusters become much more important in liquid metals than in substitutional alloys, and that the pair TCA, which seems to do quite a nice job for substitutional alloys, has a curiously distorting effect in the fluid case. It now appears that a much greater degree of self-consistency may be achieved by deviating from the pure MCA expansion, and work is now in progress to see what can be done in this way.

It is important to understand the characteristics of the TCA in the case of fluids, so that we can see what still must be accomplished in order to treat cluster effects satisfactorily. The ultimate goal, a satisfactory cluster approximation including short-range order, seems to be even further away.

ACKNOWLEDGMENTS

This research was sponsored in part by the Division of Materials Sciences and Applied Mathematical Sciences Research Program, Office of Energy Research, U.S. Department of Energy under Contract No. W-7405-eng-26 with Union Carbide Corporation. Two of the authors (A.K.S. and R.M.) gratefully acknowledge the hospitality and support that they received as guests of the Solid State Division and the Metals and Ceramics Division, respectively, of Oak Ridge National Laboratory. The authors especially wish to thank William H. Butler for helpful discussions and (as mentioned in Ref. 4) for the use of the computer program developed for numerical simulation of the one-dimensional δ-function fluid. Oak Ridge National Laboratory was, at that time, being operated by Union Carbide Corporation under Contract W-7405-eng-26 with the U.S. Department of Energy.

APPENDIX A: AUGMENTED SPACE FORMALISM

Here we develop the machinery for applying the TCA logic to an uncorrelated gas of scatterers. By treating the scatterers as infinitely massive noninteracting bosons, and describing their configurations by means of creation and annihilation operators, we convert configuration averages to expectation values. The configuration average for the uncorrelated system is obtained by taking an expectation value in the degenerate boson ground state. With the usual c-number substitution for the annihilation and creation operators of the macroscopically occupied state, we can use the basis of excitations above that ground state, which we may call "pseudobosons," as a convenient basis for a perturbative expansion of the ground-state expectation value. An m-site TCA is obtained by restricting this basis to a maximum of m pseudoboson excitations.

Let $b_x^\dagger$ create a scatter at x. Then the configuration $\underline{x}$ corresponds to the state

$$|\underline{x})) = \frac{1}{(N!)^{1/2}} \prod_1^N b_{x_i}^\dagger |\text{vac})) . \tag{A1}$$

Here, we are representing the scatterer states by vectors in a Fock space $\mathscr{F}'$. The full augmented space is given by the outer product $\mathscr{S} = \mathscr{H} \otimes \mathscr{F}'$, where $\mathscr{H}$ is the Hilbert space of the original Hamiltonian as discussed in Sec. II.

If $V_{\underline{x}}$ is the potential for a configuration $\underline{x} \equiv \{x_i\}$,

$$V_{\underline{x}} = \sum_{i=1}^N v_{x_i} , \tag{A2}$$

then the mean resolvent is

$$G^c = \langle G_{\underline{x}} \rangle = \langle [(G^0)^{-1} - V_{\underline{x}}]^{-1} \rangle . \tag{A3}$$

With an interaction of the form

$$\mathscr{V} = \int dx\, b_x^\dagger v_x b_x , \tag{A4}$$

we obtain $G_{\underline{x}}$ as the expectation value,

$$((\underline{x} \mid \mathscr{G} \mid \underline{x}')) = G_{\underline{x}} \delta_s(\underline{x}, \underline{x}') , \tag{A5}$$

where

$$\mathscr{G} = [(G^0)^{-1} - \mathscr{V}]^{-1} \tag{A6}$$

and

$$\delta_s(\underline{x}, \underline{x}') = ((\underline{x} \mid \underline{x}')) , \tag{A7}$$

the symmetrized δ function. Here the symbol G^0 actually represents $G^0 \otimes I_{\mathscr{F}'}$, where $I_{\mathscr{F}'}$ is the unit operator in the Fock space, $\mathscr{F}'$. We suppress this $I_{\mathscr{F}'}$ in similar expressions below.

The creation operator for the momentum state k is

$$\hat{b}_k^\dagger = \frac{1}{\Omega^{1/2}} \int e^{ik \cdot x} b_x^\dagger dx , \tag{A8}$$

where Ω is the normalization volume.

The degenerate ground state, which is the pseudoboson "vacuum" state, is the reference state for the TCA analysis, and is given by

$$|\phi\rangle = \frac{1}{(N!)^{1/2}} (\hat{b}_0^\dagger)^N |\text{vac})) = \frac{1}{\Omega^{N/2}} \int d^N x\, |\underline{x})) . \tag{A9}$$

Since the bosons have no dynamics, an expectation value in state $|\phi\rangle$ constitutes simply an average over configuration $\underline{x}$:

$$G^c = \langle \phi \mid \mathscr{G} \mid \phi \rangle = \frac{1}{\Omega^N} \int d^N x\, G_{\underline{x}} . \tag{A10}$$

In the macroscopic limit $N \to \infty$, $n = N/\Omega = \text{constant}$, we can make the standard c-number substitution (Mills[22])

$$\hat{b}_0 = \hat{b}_0^\dagger = \sqrt{N} , \tag{A11}$$

so that

$$b_x = \frac{1}{\Omega^{1/2}} \sum_k \hat{b}_k e^{ik \cdot x} = (\sqrt{n} + a_x) , \tag{A12}$$

where

$$a_x = \frac{1}{\Omega^{1/2}} \sum_{k(\neq 0)} \hat{b}_k e^{ik \cdot x} . \tag{A13}$$

a_x lacks the $k = 0$ component, so that

$$a_x |\phi\rangle = 0 . \tag{A14}$$

Thus $|\phi\rangle$ is a ground state with respect to the pseudoboson excitations $a_x^\dagger$. The interaction (A4) can now be written as

$$\mathscr{V} = \int dx (\sqrt{n} + a_x^\dagger) v_x (\sqrt{n} + a_x) . \tag{A15}$$

The vectors in the new Fock space $\mathscr{F}$ are $|\phi\rangle$, the pseudoboson vacuum, $|x\rangle = a_x^\dagger |\phi\rangle$, the one pseudoboson excitation, and so forth. The general state $|\underline{x}\rangle$ is labeled by the set $\underline{x}$ of occupied locations x_i:

$$|\underline{x}\rangle = \frac{1}{(r!)^{1/2}} \prod_{x_i \in \underline{x}} a_{x_i}^\dagger |\phi\rangle , \tag{A16}$$

where r is the order of $\underline{x}$. Graphically the pseudobosons are represented by horizontal lines, logically equivalent, in fact, to the MCA ("modified cumulant average") lines of the TCA for substitutional alloys.[10] In a perturbative expansion, successive virtual pseudoboson states appear from right to left, as shown in a typical case in Fig. 9. The set $\underline{x}$ characterizing the successive pseudoboson states are referred to as overlap sets.

Following MR, let us now define the projection operator Q onto the non-null overlap sets of the Fock space $\mathscr{F}$:

$$Q = I_{\mathscr{F}} - |\phi\rangle\langle\phi| . \tag{A17}$$

Then

$$[(G^0)^{-1} - \mathscr{V}] = [(G^0)^{-1} - Q\mathscr{V}] - |\phi\rangle\langle\phi|\mathscr{V} . \tag{A18}$$

Multiplying both sides of (A18) by $\langle\phi| [(G^0)^{-1} - \mathscr{V}]^{-1}$ on the left and by $[(G^0)^{-1} - Q\mathscr{V}]^{-1} |\phi\rangle$ on the right, and using (A6) and (A10), one gets

$$\langle\phi| [(G^0)^{-1} - Q\mathscr{V}]^{-1} |\phi\rangle = G^c - G^c \langle\phi| \mathscr{V} [(G^0)^{-1} - Q\mathscr{V}]^{-1} |\phi\rangle , \tag{A19}$$

from which, by the property

$$\langle\phi| Q = 0 \tag{A20}$$

of Q, one has

$$G^0 = G^c - G^c \langle\phi| \mathscr{V} (1 - G^0 Q \mathscr{V})^{-1} |\phi\rangle G^0 \tag{A21}$$

or

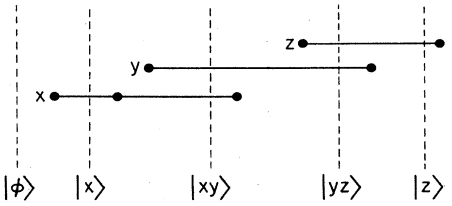

FIG. 9. Virtual pseudoboson states in a typical graph in the expansion of V^c.

$$G^c=[(G^0)^{-1}-V^c]^{-1}\ , \tag{A22}$$

where

$$V^c=\langle\phi\,|\,\mathscr{V}(1-G^0Q\mathscr{V})^{-1}\,|\,\phi\rangle$$
$$=\langle\phi\,|\,(\mathscr{V}^{-1}-G^0Q)^{-1}\,|\,\phi\rangle\ , \tag{A23}$$

the coherent potential, expressed as an augmented space expectation value [cp. MR, Eq. (A16)]. But the expression in (A23) contains Q, which comprises an infinite number of possible overlap sets. The TCA(m) for fluids consists in limiting Q to overlap sets up to some finite maximum order m, that is,

$$Q\simeq Q_m=\sum_{r=1}^{m}P_r\ , \tag{A24}$$

where P_r, given by

$$P_r=\int|x_1,x_2,\ldots,x_r\rangle\langle x_1,x_2,\ldots,x_r\,|\,d^Nx\ , \tag{A25}$$

is the projector onto the space of r pseudoboson states. Thus in this approximation,

$$V^c=\langle\phi\,|\,(\mathscr{V}^{-1}-Q_mG^0)^{-1}\,|\,\phi\rangle\ . \tag{A26}$$

Now comes the question of introducing self-consistency in the manner described in Sec. II. According to that prescription, we have to replace Q_mG^0 [for TCA(m)] by

$$\mathscr{G}_m=Q_{m-1}G^0+P_mG^c\ . \tag{A27}$$

Thus, for TCA(m), we have

$$V^c=\langle\phi\,|\,(\mathscr{V}^{-1}-\mathscr{G}_m)^{-1}\,|\,\phi\rangle\ . \tag{A28}$$

APPENDIX B: THE FIXED-POINT THEOREM FOR THE FLUID TCA

In (A28), $\mathscr{G}_m$ depends on G^c, which in turn depends on V^c. Thus, the right-hand side of (A28) may be written as a functional $F[V^c]$, and we get the fixed-point equation

$$V^c=F[V^c]\ , \tag{B1}$$

where

$$F[V^c]=\langle\phi\,|\,(\mathscr{V}^{-1}-Q_{m-1}G^0-P_mG^c(V^c))^{-1}\,|\,\phi\rangle\ . \tag{B2}$$

Starting with an initial guess V_0^c, our goal is to show that for any complex E ($\mathrm{Im}E\neq0$), $V_n^c=F[V_{n-1}^c]$ converges to the desired solution as $n\to\infty$.

We first introduce the notation

$$(\mathscr{V}^{-1}-\mathscr{G}_m)^{-1}=\mathscr{V}+\mathscr{V}\Gamma\mathscr{V}\ , \tag{B3}$$

where

$$\Gamma=(\mathscr{G}_m^{-1}-\mathscr{V})^{-1}\ , \tag{B4}$$

and $\mathscr{G}_m^{-1}$, like all such inverses appearing below, is defined on the subspace $\mathscr{S}^{(m)}=Q_m\mathscr{S}$.

$$F[V^c]=\langle\phi\,|\,\mathscr{V}(1+\Gamma\mathscr{V})\,|\,\phi\rangle\ . \tag{B5}$$

The norm $||A||$ of an operator A is defined as

$$||A||=\sup_{\psi}\frac{||A\psi||}{||\psi||}\ , \tag{B6}$$

and thus from (B5), by the usual properties of the norm,

$$||F[V^c]||\leq||\mathscr{V}||\ \ (1+||\Gamma||\,||\mathscr{V}||)\ . \tag{B7}$$

We can use the same pattern of proof as in the substitutional alloy case,[10] but in order to do so we need to establish five points:

(i) $\mathscr{V}$ is a Hermitian operator, i.e., $\mathscr{V}=\mathscr{V}^\dagger$. This follows directly from Eq. (A15).

(ii) If $V^c(E)$ is taken to have the Herglotz property, then $F[V^c(E)]$ is also Herglotz. This can be seen by inspection of Eq. (B2).

(iii) $-L_0(E)$ is a Herglotz operator valued function of E, which need not be bounded.

(iv) For D a compact subset of the upper half $\mathscr{I}_+$ of the complex E plane, $\mathrm{Im}L_0(E)$ has a uniform lower bound $y>0$ in D, namely

$$y=\inf_D\mathrm{Im}E\ .$$

(v) V_x is a bounded operator on $\mathscr{H}$: the derived operator $\mathscr{V}$ is therefore a bounded operator on $\mathscr{S}$. This point is nontrivial; its proof makes up the bulk of what follows.

From the definition of the norm,

$$||\Gamma||^2=\sup_{\varphi}\left[\frac{\bar{\varphi}\bar{\Gamma}\Gamma\varphi}{\bar{\varphi}\varphi}\right]$$
$$=\sup_{\psi}\left[\frac{\bar{\psi}\psi}{\bar{\psi}\bar{\mathscr{L}}\mathscr{L}\psi}\right]=\sup_{\psi}\left[\frac{1}{\bar{\psi}\bar{\mathscr{L}}\mathscr{L}\psi}\right]\ , \tag{B8}$$

where

$$\psi=\Gamma\varphi \tag{B9}$$

can be taken as normalized, and

$$\mathscr{L}=\Gamma^{-1}=(\mathscr{G}_m^{-1}-\mathscr{V})\ . \tag{B10}$$

Now for any normalized vector x and any operator A,

$$|\langle x\,|\,A\,|\,x\rangle|\leq||A||\ , \tag{B11}$$

so that

$$\bar{\psi}\bar{\mathscr{L}}\mathscr{L}\psi\geq|\bar{\psi}\mathscr{L}\psi|^2\geq|\bar{\psi}\mathscr{L}_I\psi|^2\ , \tag{B12}$$

where $\mathscr{L}_I$ is the anti-Hermitian part of $\mathscr{L}$. Thus, from (B8),

$$||\Gamma||\leq\frac{1}{\inf_{\psi}|\bar{\psi}\mathscr{L}_I\psi|}\ . \tag{B13}$$

Now, let us note that from (A29), and using the orthogonality of Q_{m-1} and P_m,

$$\mathscr{G}_m^{-1}=Q_{m-1}L_0+P_m(G^c)^{-1} \tag{B14}$$
$$=Q_mL_0-P_mV^c\ . \tag{B15}$$

Thus since $V^c(E)$ has the Herglotz property and $\mathscr{V}$ is Hermitian,

$$\mathscr{L}_I = \mathrm{Im}\mathscr{G}_m^{-1} \geq Q_m \mathrm{Im} L_0 \geq y \ , \tag{B16}$$

in the subspace $\mathscr{S}^{(m)}$, and

$$||\Gamma|| \leq \frac{1}{y} \ . \tag{B17}$$

Next, we want to look at

$$||\mathscr{V}|| = \sup_{||\psi||=1} (\bar{\psi}\mathscr{V}\psi) \ .$$

Let us label the vectors in the augmented space $\mathscr{S} = \mathscr{H} \otimes \mathscr{F}$ as $|\underline{x}, r\rangle$; where $\underline{x}$ denotes the overlap set $\{x_i\}$, $i = 1, \ldots, \nu$ $(0 \leq \nu \leq m$, the order of the approximation), and r denotes the electron's position. We also write

$$(r \mid \psi\rangle = \varphi(r) \in \mathscr{F} \ . \tag{B18}$$

$$= \sum_{\nu} \int d^{\nu}x \, |\underline{x}\rangle\langle \underline{x}, r \mid \psi\rangle = \sum_{\nu} \varphi_{\nu}(r) \ , \tag{B19}$$

where

$$\varphi_{\nu}(r) = \int d^{\nu}x \, |\underline{x}\rangle\langle \underline{x}, r \mid \psi\rangle \ . \tag{B20}$$

From the definition (A15) of $\mathscr{V}$,

$$\bar{\psi}\mathscr{V}\psi = n \int dx \, \bar{\psi} V_x \psi + \sqrt{n} \int dx \, \bar{\psi} V_x a_x \psi + \sqrt{n} \int dx \, \bar{\psi} a_x^{\dagger} V_x \psi + \int dx \bar{\psi} a_x^{\dagger} V_x a_x \psi \tag{B21}$$

$$\equiv I_1 + I_2 + I_3 + I_4 \ . \tag{B22}$$

Since V_x can be expressed as the difference of two positive semidefinite operators, both of which will be bounded, it is sufficient to treat the case that V_x is positive semidefinite. Let us first find upper bounds for the terms I_1 and I_4:

$$\begin{aligned} |I_1| &= |n \int dx \, \bar{\psi} V_x \psi| \\ &= n \left| \int dx \int dr' \int dr'' \langle \psi \mid r')(r' \mid V_{\vec{x}} \mid r'')(r'' \mid \psi\rangle \right| \\ &= n \left| \int dx \int dr' v(r'-x) ||\varphi(r')||^2 \right| \\ &= n \int v(r) dr \int ||\varphi(r')||^2 dr' \\ &= n \left| \int dr \, v(r) \right| \leq c_1 \ , \end{aligned} \tag{B23}$$

where Eq. (2.3) has been used, and the potential due to the scatterer is assumed bounded and integrable.

Now, let

$$\sup_r v(r) = v_0 \ .$$

Then

$$\begin{aligned} I_4 &= \int dx \int dr \int dr' \langle \psi \mid r)(r \mid a_x^{\dagger} V_x a_x \mid r')(r' \mid \psi\rangle \\ &= \int dx \int dr \, v(r-x) \bar{\varphi}(r) a_x^{\dagger} a_x \varphi(r) \\ &= \int dr \, v(r) \int dx \, \bar{\varphi}(r+x) a_x^{\dagger} a_x \varphi(r+x) \\ &\leq v_0 \sum_{\nu=0}^{m} \int \bar{\varphi}_{\nu}(r+x) a_x^{\dagger} a_x \varphi_{\nu}(r+x) dr \, dx \ . \end{aligned} \tag{B24}$$

It may be noted here that this step is not valid for our model δ-function potential, since $v(r) = \delta(r)$, which is not bounded. However, the theorem is applicable to a wide class of realistic potentials. Even for the δ-function potential, we tested our computation with many possible initial values of $V^c(k)$, and the Herglotz property (physical behavior) was never seen to be violated, either for TCA(1) $\equiv$ CPA or for TCA(2). Presumably, the proof of the fixed-point theorem for this model potential has to be slightly different, or perhaps exceptions could be found using extreme forms for the initial $V^c(k)$.

Now

$$\langle \underline{x}' \mid a_x^{\dagger} a_x \mid \underline{x}'' \rangle = \delta_{\nu'\nu''} \delta_s(\underline{x}', \underline{x}'') \sum_{i=1}^{\nu'} \delta(x - x_i') \ , \tag{B25}$$

where ν' and ν'' represent the order of the overlap sets $\underline{x}'$ and $\underline{x}''$, respectively, and δ_s is the symmetrized δ function defined by (A7). Thus

$$\begin{aligned} \int \bar{\varphi}_{\nu}(r+x) a_x^{\dagger} a_x \varphi_{\nu}(r+x) dx \, dr &= \int d^{\nu}x' d^{\nu}x'' \langle \psi \mid \underline{x}', r+x\rangle\langle \underline{x}' \mid a_x^{\dagger} a_x \mid \underline{x}''\rangle\langle \underline{x}'', r+x \mid \psi\rangle dx \, dr \\ &= \int |\langle \underline{x}', r+x \mid \psi\rangle|^2 \sum_{i=1}^{\nu} \delta(x - x_i') d^{\nu}x' \, dx \, dr \\ &= \sum_{i=1}^{\nu} \int d^{\nu}x' dr \, |\varphi_{\nu}(x', r+x_i')|^2 \ . \end{aligned} \tag{B26}$$

Now, for each ν,

$$\int |\varphi_{\nu}(x, r)|^2 d^{\nu}x \, dr \leq ||\psi||^2 \leq 1 \ .$$

Thus

$$\int \bar{\varphi}_{\nu}(r+x) a_x^{\dagger} a_x \varphi_{\nu}(r+x) dx \, dr \leq \nu \ ,$$

and hence from (B24)

$$I_4 \leq v_0 \sum_{\nu=0}^{m} \nu = c_4 \ .$$

Now as to I_2 and I_3 [Eq. (B22)], with the restriction $V_x \geq 0$ discussed above, and with the observation that both $\langle \mathscr{V} \rangle$ and $\langle \mathscr{V}' \rangle$, where

$$\begin{aligned} \langle \mathscr{V}' \rangle &= \bar{\psi}(\sqrt{n} - a_x^{\dagger}) V_x (\sqrt{n} - a_x) \psi \\ &= I_1 - I_2 - I_3 + I_4 \ , \end{aligned} \tag{B27}$$

are non-negative, we see immediately that

$$|I_2+I_3|<I_1+I_4\leq c_1+c_4\ ,$$

so that $\bar{\psi}\mathscr{V}\psi$ is bounded. The restriction that V_x be positive semidefinite can now be dropped, and we write

$$||\mathscr{V}||\equiv\beta<\infty\ . \tag{B28}$$

Thus, from (B7), (B17), and (B28), one obtains

$$||F[V^c]||\leq\beta+\frac{\beta^2}{y}\equiv\gamma\ , \tag{B29}$$

and $||F[V^c]||$ is uniformly bounded for $V^c\in\mathscr{S}_-$ (Herglotz property), $E\in D$ (where $D\subset\mathscr{S}_+$) and $\mathscr{V}$ Hermitian. Having established this, the rest of the proof goes through exactly as in MR, and is not given here to avoid repetition. The conclusion is that if m,n are the order of iteration of the fixed-point equation such that $n>m$, then

$$||V_n^c-V_m^c||\to 0\ \ (m,n\to\infty)\ , \tag{B30}$$

and the sequence $\{V_n^c\}$ has a uniform limit $V^c(E)$. Furthermore, if $V_0^c(E)$ is an operator-valued analytic function, then so is each $V_n^c(E)$, and thus the limit $V^c(E)$ is analytic in D.

[1]H. L. Frisch and S. P. Lloyd, Phys. Rev. **120**, 1175 (1960).
[2]T. Fujiwara and Y. Tanabe, J. Phys. F **9**, 1085 (1979).
[3]M. Lax and J. C. Phillips, Phys. Rev. **110**, 41 (1958).
[4]H. K. Peterson, L. M. Schwartz, and W. H. Butler, Phys. Rev. B **11**, 3678 (1975). The authors are grateful to Dr. Butler for making the program available to them.
[5]J. S. Faulkner, Phys. Rev. B **1**, 934 (1970).
[6]L. Huisman, D. Nicholson, L. Schwartz, and A. Bansil, Phys. Rev. B **24**, 1824 (1981).
[7]J. R. Klauder, Ann. Phys. (N.Y.) **14**, 43 (1961).
[8]L. M. Roth, Phys. Rev. B **9**, 2476 (1974).
[9]V. A. Singh, Phys. Rev. B **24**, 4852 (1981).
[10]R. Mills and P. Ratanavararaksa, Phys. Rev. B **18**, 5291 (1978).
[11]P. Soven, Phys. Rev. **156**, 809 (1967); D. W. Taylor, *ibid.* **156**, 1017 (1967).
[12]D. M. Nicholson and L. Schwartz, Phys. Rev. Lett. **49**, 1050 (1982).
[13]D. M. Nicholson *et al.*, Solid State Commun. **46**, 891 (1983).
[14]D. M. Nicholson *et al.*, Phys. Rev. B **29**, 1633 (1984).
[15]T. Kaplan, P. L. Leath, L. J. Gray, and H. W. Diehl, Phys. Rev. B **21**, 4230 (1980).
[16]B. G. Nickel and J. A. Krumhansl, Phys. Rev. B **4**, 4354 (1971).
[17]R. Mills, Phys. Rev. B **8**, 3650 (1973).
[18]T. Kaplan and L. J. Gray, Phys. Rev. B **14**, 3462 (1976).
[19]A. Mookerjee, J. Phys. C **6**, L205 (1973); **6**, 1340 (1973).
[20]L. J. Gray and T. Kaplan, Phys. Rev. B **24**, 1872 (1981).
[21]B. G. Nickel and W. H. Butler, Phys. Rev. Lett. **30**, 373 (1973).
[22]R. Mills, Phys. Rev. A **4**, 394 (1971).